INT. J. REMOTE SENSING, 1991, VOL. 12, NO. 3, 643–649

Airborne remote sensing of canopy water thickness scaled from leaf spectrometer data

E. RAYMOND HUNT, JR

School of Forestry, University of Montana, Missoula, Montana 59812, U.S.A.

(Received 7 August 1990; in final form 1 November 1990)

Abstract. The reflectance ratio of the middle-infrared band (MIR, 1·55–1·75 μm) to the near-infrared band (NIR, 0·76–0·90 mm) is linearly related to the $\log_{10}$ equivalent water thickness (EWT) for single leaves of different morphologies, whereas the MIR/NIR radiance ratio is correlated with the leaf area index (LAI). The hypothesis that the MIR/NIR ratio measures canopy EWT was tested by reanalysing airborne Thematic Mapper Simulator and field data obtained across a large gradient of LAI in western Oregon, U.S.A. The measured airborne MIR/NIR reflectance ratios for canopies were not significantly different from the predicted ratios using leaf data for canopy EWT, except for two desert woodland sites. The interpretation of the MIR/NIR ratio is scale-dependent, because leaf EWT is determined by physiology, whereas canopy EWT is determined primarily by variations in LAI.

1. Introduction

Leaf reflectances of optical–infrared wavelengths from 1·1 μm to 2·5 μm are dominated by the liquid water absorption spectrum (Gates 1980). Reflectance of a middle-infrared band (MIR, 1·55–1·75 μm, equivalent to Landsat Thematic Mapper band 5) is largely determined by the optical depth of water in a single leaf according to the Beer-Lambert law. The ratio of reflectance at 1·65 μm to the reflectance at 0·82μm in the near-infrared is highly correlated to the water content of single leaves (Hunt and Rock 1989). Because low leaf water contents are indicative of plant water stress (and possibly high transpiration rates), there has been much research on relating leaf water content to optical–infrared reflectance and various remotely sensed vegetation indices. However, recent work has shown the ratio of MIR to a near-infrared band (NIR, 0·76–0·90 μm, equivalent to Landsat Thematic Mapper band 4) and other indices may not be able to detect low leaf water contents associated with plant water stress (Hunt and Rock 1989, Bowman 1989, Pierce *et al.* 1990, Riggs and Running 1991).

The ratio of MIR to NIR (or its reciprocal) is also highly correlated with the leaf area index (Curran and Williamson 1987, Peterson *et al.* 1990). It was hypothesized that this index is correlated to the LAI through the summation of the individual leaf equivalent water thicknesses (EWT = leaf water volume/projected leaf area) for each leaf layer to obtain a total canopy equivalent water thickness, which can be considered as the depth of water in the foliage. This hypothesis was tested by reanalysing field and airborne Thematic Mapper Simulator data from Running *et al.* (1986) and Peterson *et al.* (1987). These data were obtained across a large gradient of LAI in western Oregon, U.S.A.; where the large differences in the LAI are caused by differences in site water balance (Grier and Running 1977, Gholz 1982). For comparison with the broad-band airborne Thematic Mapper Simulator data, laboratory reflectance data from Hunt and Rock (1989) were reanalysed to determine the relationship of EWT to MIR/NIR for single leaves of various morphologies.

2. Methods

2.1. *Laboratory data*

Reflectance spectra of leaves from a leaf succulent *Agave deserti* (agave, number n of leaves $= 10$), a crop plant *Glycine max* (soybean, $n = 12$), a broadleaf tree species *Liquidambar styraciflua* (sweet gum, $n = 15$), a schlerophyll *Quercus agrifolia* (California live oak, $n = 10$), and conifers *Picea rubens* (red spruce, $n = 4$) and *P. pungens* (blue spruce, $n = 4$) were measured with a Beckman UV 5240 spectrometer (Irvine, California, U.S.A.) at various times as the leaves dried on a laboratory bench (Hunt and Rock 1989). The leaf fresh weight (FWT) was measured with each reflectance; after the experiment, the leaf dry weight (DWT) and the projected leaf area were determined. The EWT was calculated as [(FWT − DWT)/area], assuming the density of liquid water is $1000\,\mathrm{kg\,m^{-3}}$.

The high-spectral resolution laboratory data were degraded to the NIR and MIR broad-band reflectances factors using an equation of Gates (1980), modified with the sensor response from Suits (1983).

$$\rho_b = \int \rho_\lambda s_\lambda E_\lambda \, d\lambda \bigg/ \int s_\lambda E_\lambda \, d\lambda$$

where ρ_b is the reflectance factor of either the NIR band (for λ from $0{\cdot}76\,\mu$m to $0{\cdot}90\,\mu$m) or the MIR band (for λ from $1{\cdot}55\,\mu$m to $1{\cdot}75\,\mu$m), ρ_λ is the reflectance factor at wavelength λ, E_λ is the radiant flux density at each wavelength and s_λ is the sensor response from 0 to 100 per cent at each λ provided by the Daedalus Enterprises, Inc. (Ann Arbor, Michigan, U.S.A.) for the Daedalus airborne Thematic Mapper Simulator bands 7 (NIR) and 9 (MIR). The radiant flux density E_λ for the Beckman spectrometer was not known, so as an approximation E_λ was taken to be the spectral solar irradiance from LOWTRAN 6 model output (Kniezys *et al.* 1983).

2.2. *Calculation of canopy equivalent water thickness*

Eighteen stands were sampled in August 1983 by Running *et al.* (1986) and Peterson *et al.* (1987) from seven coniferous vegetation zones from the western coast range to the interior high desert across an east-west transect in western Oregon, U.S.A. (latitude $\approx 44{\cdot}5°$ N). The project LAI was estimated from either tree diameters at a height of 1·3 m (Running *et al.* 1986) or sapwood basal areas for some stands of *Pseudotsuga menzeisii* and *Pinus ponderosa* (Peterson *et al.* 1987). LAI's of stands 9, 11 and 12 in Peterson *et al.* (1987) were probably overestimated; using the data of Marshall and Waring (1986), their overstory LAI's were estimated to be 11, 9 and 9, respectively.

In June 1990, six of the 18 stands were sampled to determine the average leaf EWT for the dominant species (see the table). Needles from different species were sealed in plastic bags and kept in the dark until the fresh weights were determined. The projected leaf area was calculated from the lengths and diameters of the needles. Then the needles were dried at 60°C for two days and their dry weights were measured. The average leaf EWT was determined for the aggregate number of needles because the weight of the individual needles was close to the precision of the balance. The EWT

Equivalent water thicknesses of dominant species in western Oregon, U.S.A. Fresh weight (FWT), dry weight (DWT) and projected area were measured for the aggregate number of needles n to determine the equivalent water thickness (EWT).

Species	n	FWT (g)	DWT (g)	area (mm^2)	EWT (mm)
Picea sitchensis	40	0·415	0·278	690	0·199
Tsuga heterophylla	50	0·633	0·211	951	0·444
Tsuga mertensiana	40	0·624	0·194	960	0·447
Pseudotsuga menzeisii	40	0·346	0·195	738	0·205
Abies amabilis	40	0·660	0·377	1035	0·273
Abies lasiocarpa	40	0·530	0·361	787	0·215
Pinus contorta	40	1·525	0·745	2580	0·302
Pinus ponderosa	42	5·111	2·436	8840	0·303
Juniperus occidentalis	20	3·240	1·407	2045	0·896

for species not in the table, or for two codominant species in Peterson *et al.* (1987), was taken to be the mean EWT of the genus or of the codominant species, respectively. The canopy EWT for each stand was calculated as the leaf EWT (see the Table) multiplied by the overstory LAI, plus the understory leaf EWT (taken to be 0·1 mm) multiplied by the understory LAI, where stand LAI's were given by Peterson *et al.* (1987).

2.3. *Airborne data reanalysis*

Daedalus airborne Thematic Mapper Simulator data were obtained along the east-west transect at about solar noon on 15 August 1983 (Peterson *et al.* 1987). The digital numbers were converted to radiances L using the instrument calibration curves, and the atmospheric path radiance L_p was determined by measuring radiances from light and dark targets using a Barnes Modular Multiband Radiometer (Peterson *et al.* 1987).

The radiances were then corrected for the solar irradiance E of Landsat Thematic Mapper bands 4 and 5 outside the atmosphere (Norwood and Lansing 1983) and the atmospheric transmittance T, to obtain reflectances of

$$\rho_b = \pi(L - L_p)/ET$$

(Badhwar *et al.* 1986). T was calculated as

$$T = \tau_b^m$$

where τ_b is the atmospheric transmissivity for either the NIR or MIR bands and m is the air mass. The transmissivity was calculated to be 0·74 and 0·83 for the NIR and MIR bands, respectively, using the LOWTRAN 6 model output (Kniezys *et al.* 1983). The air mass was determined according to Gates (1980) as

$$m = (p/p_0) \operatorname{secant} z$$

where p is the approximate atmospheric pressure determined from stand elevation, p_0 is the pressure at sea level (taken to be 101·3 kPa) and z is the solar zenith angle. Other factors, such as the site slope and aspect, tend to affect both bands equally and were not considered further.

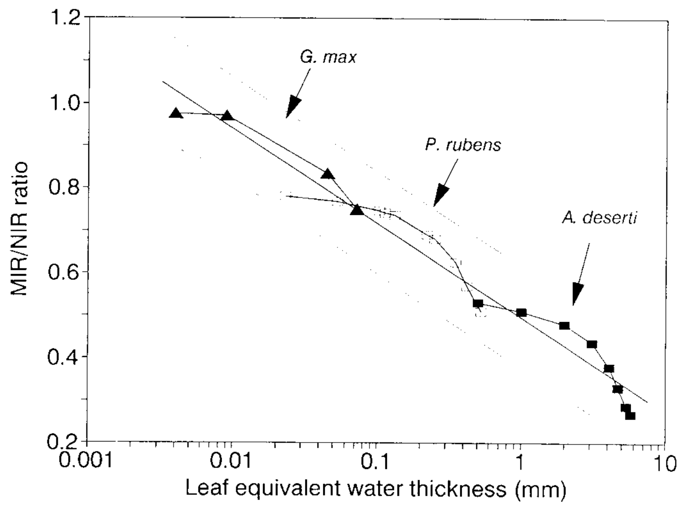

Figure 1. Reflectance ratio of middle-infrared band (MIR, 1·55–1·75 μm) to near-infrared band (NIR, 0·76–0·90 μm) for single leaves compared to their equivalent water thickness (EWT). The abscissa is a log scale to accommodate the four orders of magnitude variation of EWT for six different species with different leaf morphologies. The least-squares regression equation (solid line) is MIR/NIR ratio $= 0{\cdot}496 - 0{\cdot}222 \log_{10}$ (leaf EWT), for 296 points from 55 leaves as they dried on a laboratory bench, $r^2 = 0{\cdot}89$, $se(\hat{y}) = 0{\cdot}061$, $se(b_0) = 0{\cdot}0054$, and $se(b_1) = 0{\cdot}0048$. The dotted lines are the ± 95 per cent confidence intervals for $\hat{y}$. The points are for single representative leaves of *Glycine max* (▲), *Picea rubens* (□), and *Agave deserti* (■) as they dried over time.

3. Results and discussion

As the EWT becomes smaller for single drying leaves, the MIR/NIR reflectance ratio first increases and then levels off (figure 1). This occurs because:

(*a*) there is little change in NIR;
(*b*) the change in MIR is largely determined by the Beer-Lambert law;
(*c*) EWT is plotted on a $\log_{10}$ scale (Hunt and Rock 1989).

However, when all of the leaf data are plotted together, the MIR/NIR ratio is linearly related to $\log_{10}$ EWT (figure 1), because thicker leaves generally have higher reflectance in the NIR and hold more water, and so have lower reflectance in the MIR. The $\log_{10}$ scale was chosen arbitrarily to accommodate four orders of magnitude difference in leaf EWT (Hunt and Rock 1989). So the linear relationship between the MIR/NIR ratio and the $\log_{10}$ indicates the general trend for leaves of different morphologies.

The MIR/NIR reflectance ratios for 14 of the 18 conifer forest stands fall inside the 95 per cent confidence intervals for the leaf data regression line, with an additional two stands falling just outside the 95 per cent confidence interval (figure 2). The expected regression equation for 'measured' versus 'predicted' canopy ratios from the leaf data is $y = b_0 + b_1 x$, where b_0 is expected to be 0·0 and b_1 is expected to be 1·0; the least-squares regression coefficients were $b_0 = -0{\cdot}32$ with an $se(b_0)$ of 0·83, and $b_1 = 1{\cdot}59$ with an $se(b_1)$ of 0·34. The alternative hypothesis of $b_0 \neq -0{\cdot}0$ was rejected using a t-test with $P = 0{\cdot}29$, and an alternative hypothesis of $b_1 \neq 1{\cdot}0$ was rejected with

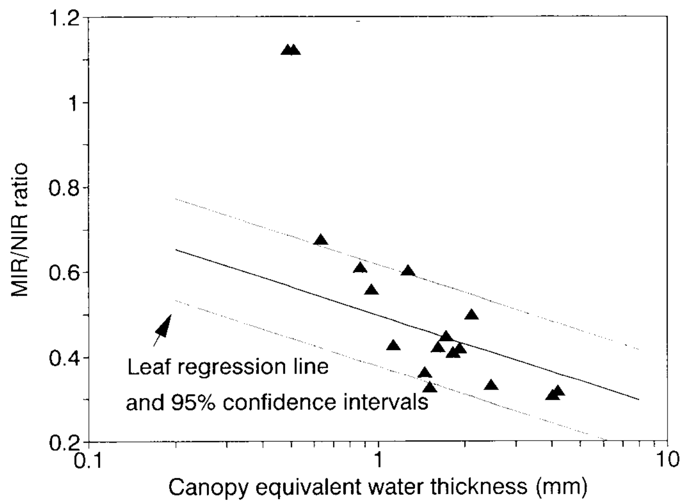

Figure 2. Reflectance ratio (▲) of middle-infrared band (MIR, 1·55–1·75 μm) to near-infrared band (NIR, 0·76–0·90 μm) versus estimated equivalent water thickness (EWT) of 18 conifer stands. The solid line is the regression equation for the leaf data and the dotted lines are the 95 per cent confidence intervals from figure 1.

$P=0{\cdot}89$. Thus, MIR/NIR for 16 of the 18 conifer stands was not significantly different from the predicted reflectance ratio determined by the canopy EWT and the leaf data regression equation in figure 1.

The MIR/NIR reflectance ratio is much higher than the leaf regression equation for two *Juniperus occidentalis* desert woodland stands (figure 2). This may be due to the high soil and dry-grass background reflectance of the NIR and MIR, in a similar manner to how the soil and dry-grass background reflectance affects NIR and red bands (Huete and Jackson 1988, Williamson 1989, Spanner *et al.* 1990). The overflight occurred in August when these woodlands typically experience summer drought (Grier and Running 1977, Gholz 1982). The open *Juniperus occidentalis* woodlands in central Oregon on the eastern side of the Cascade mountains form a very sparse canopy cover, so the influence of dry soil and grass may be particularly important for the MIR/NIR ratio (Spanner *et al.* 1990). The effects of canopy structure and shadows were not accounted for and may explain some of the variation in figure 2, however the Oregon transect study was designed to minimize the variation in canopy structure by using only coniferous stands.

Changes of MIR/NIR ratios of the order of 0·061 (the $se(\hat{y})$ in figure 1) are more likely to result from changes in the LAI over a region and at different times of the year than from a change in the leaf relative water content (defined as leaf EWT / maximum leaf EWT). A canopy would have to lose about 50 per cent of its water before a significant change in the ratio MIR/NIR would be detectable (Hunt and Rock 1989), whereas water-stressed leaves would generally lose about 15 per cent of its water. It is possible to remotely sense canopy relative water content directly (Hunt *et al.* 1987), but it is not practical (Hunt and Rock 1989).

Using high-spectral-resolution aircraft or satellite sensors, estimates of canopy EWT will be much more accurate (Gao and Goetz 1990). Even assuming these high-resolution sensors can exactly determine the changes of canopy EWT at two different times, one cannot distinguish *a priori* between lower leaf relative water contents caused by water stress and those caused by fewer layers of leaves. Moreover, drought stress usually inhibits growth and hastens leaf senescence (Hsiao 1973), so differences in LAI may be more important for the remote sensing of drought-affected areas than changes of leaf RWC. Therefore, it is unlikely that plant water stress can be detected by canopy EWT without field or other remotely sensed data.

In conclusion, the relationship between MIR/NIR reflectance ratios and the EWT from leaf spectrometer data was extrapolated to airborne Thematic Mapper Simulator data. These analyses also indicate that the MIR/NIR reflectance ratio for canopies is related to the LAI, not the leaf physiology, owing to the change in scale from leaf EWT to canopy EWT. Scaling leaf physiological variables determined with laboratory spectrometer data over large areas using remote sensing may be difficult because of the sensivity of vegetation indices to the leaf area index.

Acknowledgments

I thank Michael A. Spanner and Steven W. Running for providing the Thematic Mapper Simulator data, recent leaf samples from the Oregon Transect and discussions on data analysis. I also thank two anonymous reviewers for their comments. Funding was provided by NASA Land Processes grant NAGW-1892.

References

BADHWAR, G. D., MCDONALD, R. B., and MEHTA, N. C., 1986, Satellite-derived leaf-area-index and vegetation maps as input to global carbon cycle models—a hierarchical approach. *International Journal of Remote Sensing*, **7**, 265–281.

BOWMAN, W. D., 1989, The relationship between leaf water status, gas exchange, and spectral reflectance in cotton leaves. *Remote Sensing of Environment*, **30**, 249–255.

CURRAN, P. J., and WILLIAMSON, H. D., 1987, GLAI estimation using measurements of red, near infrared, and middle infrared radiance. *Photogrammetric Engineering and Remote Sensing*, **53**, 181–186.

GATES, D. M., 1980, *Biophysical Ecology* (New York: Springer-Verlag).

GHOLZ, H. L., 1982, Environmental limits on aboveground net primary production, leaf area, and biomass in vegetation zones of the Pacific northwest. *Ecology*, **63**, 469–481.

GAO, B.-C., and GOETZ, A. F. H., 1990, Column atmospheric water and vegetation liquid water retrievals from airborne imaging spectrometer data. *Journal of Geophysical Research*, **95**, 3549–3564.

GRIER, G. C., and RUNNING, S. W., 1977, Leaf area of mature northwestern coniferous forests: relation to site water balance. *Ecology*, **58**, 893–899.

HSIAO, T. C., 1973, Plant responses to water stress. *Annual Review of Plant Physiology*, **24**, 519–570.

HUETE, A. R., and JACKSON, R. D., 1988, Soil and atmosphere influences on the spectra of partial canopies. *Remote Sensing of Environment*, **25**, 89–100.

HUNT, E. R., JR, and ROCK, B. N., 1989, Detection of changes in leaf water content using near- and middle-infrared reflectances. *Remote Sensing of Environment*, **30**, 43–54.

HUNT, E. R., JR, ROCK, B. N., and NOBEL, P. S., 1987, Measurement of leaf relative water content by infrared reflectance. *Remote Sensing of Environment*, **22**, 429–435.

KNEIZYS, F. X., SHETTLE, E. P., GALLERY, W. O., CHETWYND, J. H., JR, ABREU, L. W., SELBY, J. E. A., CLOUGH, S. A., and FENN, R. W., 1983, Atmospheric transmittance/radiance: computer code LOWTRAN 6. Technical Report AFGL-TR-83-0187, Air Force Geophysics Laboratory, Hanscom Air Force Base, Massachusetts, U.S.A.

MARSHALL, J. D., and WARING, R. H., 1986, Comparison of methods of estimating leaf-area index in old-growth Douglas-fir. *Ecology*, **67**, 975–979.

NORWOOD, V. T., and LANSING, J. C., JR, 1983. Electro-optical imaging sensors. In *Manual of Remote Sensing, Vol. 1: Theory, Instruments and Techniques*, edited by R. N. Colwell, D. S. Simonett and F. T. Ulaby (Falls Church, Va.: American Society of Photogrammetry), (second edition), pp. 335-367.

PETERSON, D. L., SPANNER, M. A., RUNNING, S. W., and TUEBER, K. B., 1987, Relationship of Thematic Mapper Simulator data to leaf area index of temperature coniferous forests. *Remote Sensing of Environment*, **22,** 323–341.

PIERCE, L. L., RUNNING, S. W., and RIGGS, G. A., 1990, Remote detection of canopy water stress in coniferous forests using the NS001 Thematic Mapper Simulator and the Thermal Infrared Multispectral Scanner. *Photogrammetric Engineering and Remote Sensing*, **56,** 579–586.

RIGGS, G. A., and RUNNING, S. W., 1991, Detection of canopy water stress in conifers using the Airborne Imaging Spectrometer. *Remote Sensing of Environment*, to be published.

RUNNING, S. W., PETERSON, D. L., SPANNER, M. A., and TEUBER, K. B., 1986, Remote sensing of coniferous forest leaf area. *Ecology*, **67,** 273–276.

SPANNER, M. A., PIERCE, L. L., PETERSON, D. L., and RUNNING, S. W., 1990, Remote Sensing of temperate coniferous forest leaf area index. The influence of canopy closure, understory vegetation and background reflectance. *International Journal of Remote Sensing*, **11,** 95–111.

SUITS, G. H., 1983, The nature of electromagnetic radiation. In *Manual of Remote Sensing, Vol. 1: Theory, Instruments and Techniques*, edited by R. N. Colwell, D. S. Simonett and F. T. Ulaby (Falls Church, Va.: American Society of Photogrammetry), (second edition), pp. 37–60.

WILLIAMSON, H. D., 1989, Reflectance from shrubs and under-shrub soil in a semiarid environment. *Remote Sensing of Environment*, **29,** 263–271.